Proceedings of the Thirty-first (2021) International Ocean and Polar Engineering Conference **www.isope.org**
Rhodes, Greece, June 20 – 25, 2021

ISBN 978-1-880653-82-1; ISSN 1098-6189

Combined performance of innovative biomimetic ship propulsion system in waves with Dual Fuel ship engine and application to short-sea shipping

Kostas Belibassakis(1) , *Sebastiaan Bleuanus*(2), *Jacques Vermeiden*(3), *Nicholas Townsend*(4)

(1) School of Naval Architecture & Marine Engineering, National Technical University of Athens, Greece.
(2) Wartsila R&D and Engineering, Marine Power Solutions, Finland
(3) Huygens Engineers, the Netherlands.
(4) Faculty of Engineering and Physical Sciences, University of Southampton, UK

ABSTRACT

Flapping-foil thrusters arranged below the hull of the ship are examined for the exploitation of energy from wave induced motions by direct conversion to useful propulsive power. In the framework of Seatech H2020 project (https://seatech2020.eu/) flapping-foil thruster propulsion innovation is examined, in combination with standard propulsion system based on optimally controlled Dual Fuel engine, aiming at an increase in fuel efficiency and radical emission reductions of NOx, SOx, CO_2 and particulate matter. In this paper the combined performance of the above systems is examined for a short-sea shipping scenario in the North Sea and two ship types. The analysis is based on a simplified approximation using data from systematic series. The results show that: (i) flapping-foil thrusters can directly convert kinetic energy from the ship motions into thrust to augment the overall propulsion in waves, (ii) additional thrust generated by the foils will enable the engine to operate in part-load without compromising vessel speed, resulting in an additional positive effect on its emission profile, and (iii) the foils can improve the dynamic stability of the ship.

KEY WORDS: augmenting ship propulsion in waves; biomimetic thruster; combined performance with ship engine;

INTRODUCTION

Research and development results concerning flapping foil thrusters, supported by extensive experimental evidence and theoretical analysis, have shown that such systems, operating under conditions of optimal wake formation, can achieve high levels of propulsive efficiency; see, e.g., Triantafyllou et al (2000, 2004), Taylor et al (2010). Additional data concerning thrust coefficient, foil flexibility and Reynolds number effects can be found in the experimental systematic study by Vermeiden et al (2012). Based on the above results, the last period biomimetic propulsors with the ability to convert wave energy directly into thrust augmentation is subject of intensive investigation.

For ships the application of bow mounted flapping-foil thrusters positioned below the waterline, which exploit the energy from the wave induced motions to generate a net positive thrust augmenting the ship propulsion, could lead to significantly reduced engine loads. A schematic presentation of biomimetic foil thruster arranged at the bow of the ship, with support for elevating/lowering the system in the water is shown in Fig.1. In real sea conditions, the ship's propulsive power demand typically increases above the corresponding value in calm water for the same speed and at the same time experience undesirable wave induced, oscillatory, heave and pitch motions. The application of flapping foil thrusters, coupled with optimally controlled Dual Fuel engine technology, is expected to yield significant fuel savings and emission reductions.

Initial research into these systems has focused on the use of passively flapping foils for augmenting propulsion by directly converting kinetic energy from ship motions to thrust and simultaneous ship motion reductions; see Rozhdestvensky & Ryzhov (2003), Naito & Isshiki (2005) and Wu et al (2019) for extensive reviews. In Belibassakis & Politis (2013) the hydrodynamic analysis of flapping wings located beneath the hull of the ship and operating as unsteady thrusters in random waves, while travelling at constant forward speed, are examined in detail. The system is investigated as an unsteady thrust production mechanism, augmenting the overall ship propulsion. The main arrangement consists of a horizontal wing in vertical motion induced by ship heave and pitch,while pitching about its own pivot axis is actively set. A vertical oscillating wing-keel is also considered in transverse oscillatory motion, which is induced by ship rolling and swaying. Ship flow hydrodynamics are modeled in the framework of linear theory and ship responses are calculated taking into account the additional forces and moments due to the above unsteady propulsion systems. Subsequently, Bockmann & Steen (2014, 2016) have demonstrated at model scale that fixed, passive and active foil thrusters in waves can reduce the resistance and heave and pitch motions when travelling at constant forward speed. More recently, Bowker et al (2020) have developed and experimentally validated a theoretical model of a free running wave propelled boat using submerged passively flapping foils, determining the change in forward speed due to the unsteady thrust from passively sprung foils. Moreover, Belibassakis & Filippas (2015) and Filippas et al (2020) have developed a nonlinear BEM approach and studied the passive and active control of oscillating hydrofoils operating as unsteady thrusters in the presence of waves and currents. This method, based on coupled ship and flapping thruster dynamics taking into account the effects of the incoming wave field in conjunction with the ship responses and actively controlled foil pitch under random wave conditions, was found to be in agreement with CFD methods and experimental data; see also De Silva & Yamaguchi (2012). The method provides a useful tool for the detailed design, assessment and control of flapping foil thrusters and shows that good performance can be achieved in sea conditions of moderate and higher severity, under optimal passive or active control. In this case, the use of flapping foils to augment the overall propulsive efficiency of ships by extracting energy from the waves (and simultaneously damping the oscillatory ship motions) could significantly contribute to improving the efficiency and safety of shipping at sea with important environmental and economic benefits.

As part of the SeaTech H2020 project (https://seatech2020.eu/), this work provides a first indication of the combined performance of flapping-foil thrusters in waves with the ship engine. Based on simplified models for the ship dynamics in waves and the performance of the biomimetic wing, in conjunction with ship engine data, this paper examines the application of flapping-foil thrusters for a short-sea shipping scenario in the North Sea for two different ship types: a ROPAX-type passenger-car ferry and a small-size Bulk Carrier. More specifically, the SeaTech H2020 project focuses on developing two symbiotic innovations, the optimally controlled dual fuel gas engine and biometric flapping foil propulsors. The objective is to demonstrate at small scale and relevan environment, and then upscale the complementary innovations with help of an Advanced Data Analytics Framework with application to short-sea shipping. By combing these technologies, the project aims to increase fuel efficiency and radically reduce NOx, SOx, CO_2 and particulate matter emissions for short sea shipping.

METHODOLOGY

To assess the application of flapping-foil thrusters for short-sea shipping a ROPAX-type passenger-car ferry (Fig. 3) and a small-size Bulk Carrier without bulbous bow (Fig. 4) are considered. The hull form particulars are presented in Table 1. For each vessel type the system performance was estimated accounting for the ship motions, propeller and foil contributions using resistance, propeller, seakeeping and flapping thruster systematic series data obtained by BEM. Then, in order to provide predictions of the expected enhancement of the combined performance and the complementary nature of the proposed ship engine and flapping thruster system in waves, a short sea shipping scenario in the North Sea is considered.

Table 1: Hull form Particulars:

	ROPAX Passenger Car Ferry	Bulk Carrier (7600DWT) (without bulbous bow)
Length, Loa (Lpp)	120m (107m)	109m
Beam, B (stern breadth)	21m (20m)	15m
Draft, T	5.3m	7m
Service speed Vs	17knots	14knots

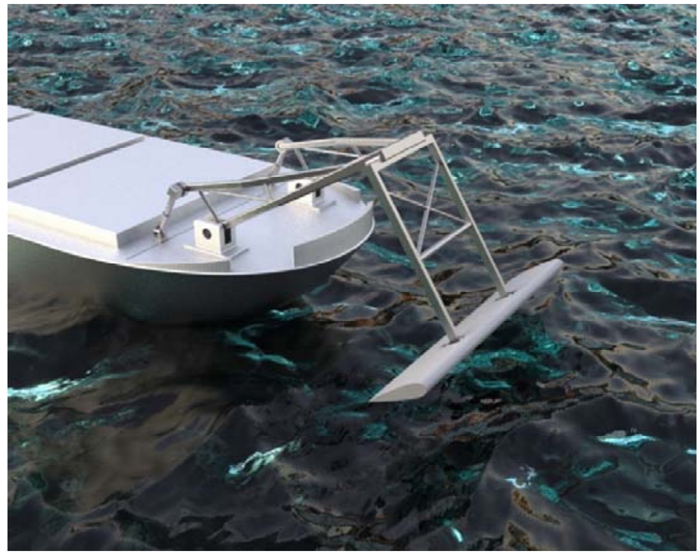

Figure 1. Illustrative representation of biomimetic thruster arranged at the bow of the ship, with support for elevating/ lowering the system in the water.

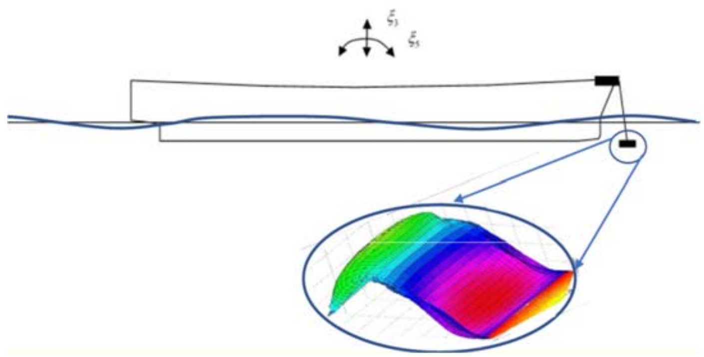

Figure 2. Ship hull in heaving and pitching motion due to waves equipped with a flapping thruster arranged below the keel, in front of the bow. The vertical foil motion is provided free of cost from ship responses, and the self-pitching motion is set by means of active or passive control. In the lower part the vorticity strength in the flapping thruster wake is shown by using color.

The present results are based on the application of systematic series, and contain an error associated with the cumulative inaccuracy of the series data. Nevertheless likely actual relationships and trend directions can be forecasted, and the present analysis is useful for the study and preliminary design of the considered system.

On the basis of the above approximations, it is indicated that additional thrust generated by the dynamic wing will enable the engine to operate in part-load without compromising vessel speed, resulting in an additional positive effect on its emission profile, and the advanced engine combustion concept is expected to contribute to energy savings and enable the retraction of the dynamic wing for safety reasons, in extreme weather conditions in order to avoid damage. Future work is planned towards the development of more accurate methods for the prediction of the combined dynamics of ship engine – biomimetic thruster performance in waves with application to a variety of ship types.

PASSENGER-CAR FERRY

This example is selected using data from Politis & Tsarsitalidis (2014, Sec.9). The estimated calm-water resistance of the ship is presented in Fig.5 as obtained using model data from NTUA towing tank rescaled to a ship of overall length 120m, corresponding to a ROPAX passenger-car ferry with main dimensions and service speed as listed in Table 1.

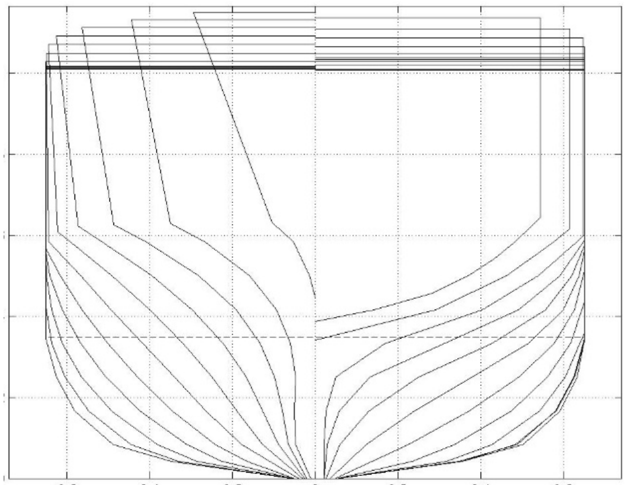

Figure 3. Body plan of the ferry (slender hull form).

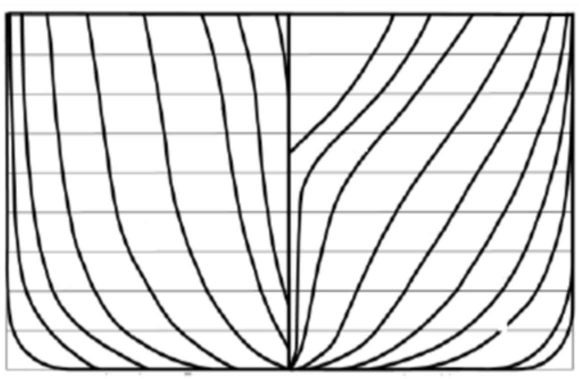

Figure 4. Body plan of the bulk carrier (full hull form).

Estimation of performance of standard propulsion system

Two propellers of diameter *D*=4m are considered for the standard propulsion system of the ferry and its performance is modeled by using B4-55 data (see Lewis 1988). For calculation purposes, the following estimated values are used for the wake fraction, thrust deduction, rotative efficiency and the shafting system efficiency: $1-t=0.95, 1-w=0.95, \eta_R=1, \eta_S=0.98$. We obtain from this example that for ship speed *V*s=17knots the optimally selected propeller pitch ratio is *P/D*=1.4, which results in SHP=4580kW (at 112RPMprop) per engine; see Fig.6. The solution is obtained by the intersection of the propeller thrust coefficient $K_T=K_T\left(J;P/D\right)$ for a given blade number and expanded area ratio with the curve of $K_T=\alpha J^2$ expressing the ship requirements

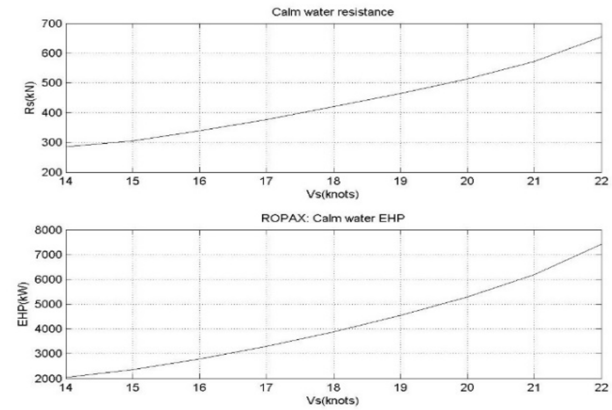

Figure 5. Calm water resistance $R_{cw}\left(V_s\right)$ and EHP curves for passenger ferry (ROPAX 120m).

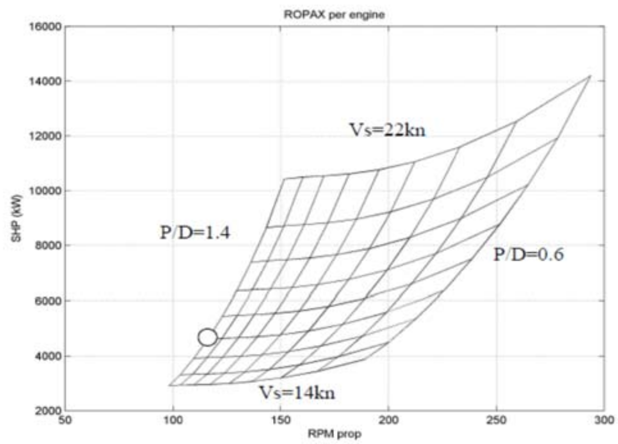

Figure 6. SHP-RPM(prop) diagram of each engine for the twin screw passenger ferry. The optimum operating point is indicated by using symbol (SHP=4580kW at 112 RPMprop).

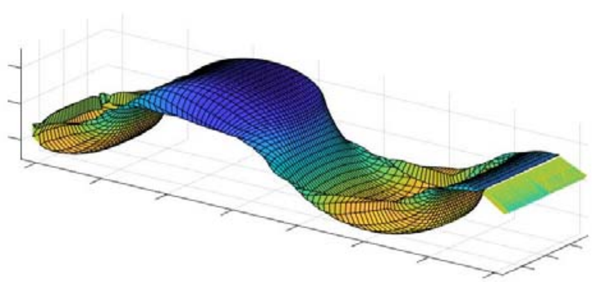

Figure 7. Plot of bow flapping thruster of orthogonal planform and the generated trailing vortex wake, as calculated by BEM vortex methods starting from rest.

$$\alpha=\frac{K_T}{J^2}=\frac{R_{tot}}{\rho\left(1-t\right)\left(1-w\right)^2 D^2 V_S^2}\ , \tag{1}$$

where ρ is the water density.

In the results presented in Fig.6 the values of the calm water resistance used are $R_{tot}=R_{cw}$. More specifically, the propeller pitch - ship speed grid is shown in Fig.6 for B4-55 propellers with *P/D*=0.6:0.1:1.4 and ship speed ranging from 14knots to 22knots.

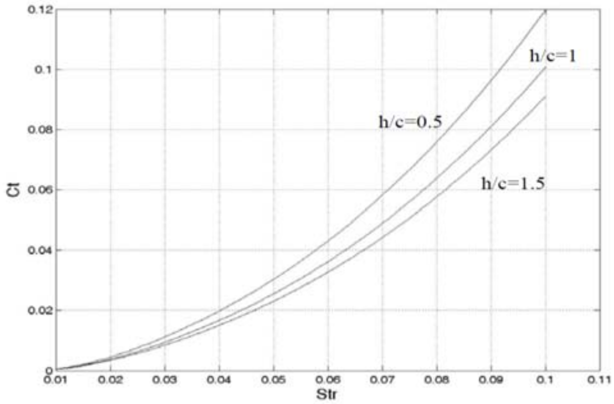

Figure 8. Thrust coefficient of the considered flapping thruster in terms of Strouhal number and heaving to chord ratio, based on data from Politis & Tsarsitalidis (2015, Fig.A17) using foil dynamic self-pitching amplitude set at θ=6deg.

In the sequel, the value of the total resistance used in the same procedure for estimating the propulsion performance will be modified as follows:

$$R_{tot} = R_{cw} + R_{add} - F_T \ , \qquad (2)$$

where R_{add} is the added wave resistance, which is dependent on the sea state and the seakeeping behaviour of the ship, and F_T the thrust offered by the flapping foil thruster operating at the bow of the ship (also dependent on wave conditions).

Ship responses in waves and flapping system performance

Detailed CFD calculations can be used to obtain data for the operation and performance characteristics of the flapping foil thruster in waves. For example, a schematic plot of the bow flapping thruster and its dynamic vortex wake development as calculated by vortex BEM is shown in Fig.7. This procedure is costly, however, at a first level of approximation a simplified approach can used to obtain demonstrative results. For the ferry heave and pitch responses at indicative sea-state conditions 4-5, corresponding to significant wave height H_s=3m and peak period T_p=8sec (see also Belibassakis & Filippas 2015, table 1) for service ship speed V_s=17knots (Froude number F_n=0.265) in head waves.

For calculating the propulsion in waves of the passenger-ferry, data from the systematic series (based on series 60) presented by Loukakis & Chryssostomidis, (1975) and extended by Grigoropoulos et al (2000) were used. From the tables in the latter works we estimate for the ferry in the considered sea-state condition 4-5:

vertical bow ship motion with rms amplitude h_0=1.35m,

which provides an estimation of the heaving amplitude of flapping thruster in waves. From the above systematic series an estimate of the mean value of added wave resistance is also obtained

R_{add}=8.5kN at the same ship speed V_s=17knots,

corresponding to about 2.5% of the calm water resistance at the same speed. By considering the added wave resistance together with the calm-water resistance it is obtained that the ferry propulsion system at V_s=17kn results in an increased power requirement: SHP=4685kW (per engine) to maintain speed.

Furthermore, for the ship travelling at this speed in head waves with peak period T_p=8sec, the encounter peak frequency is $f_e = 0.21$Hz and the corresponding period drops to 4.7s. Using a bow flapping wing thruster with chord c=2.5m and span-to-chord ratio s/c=6 (which is compatible with the breadth of the ship at a forward station of the ferry), the Strouhal number of the flapping thruster is $Str = 0.066$. In this condition, we obtain the following prediction concerning the performance of flapping thruster using data from Politis & Tsarsitalidis (2015, Fig.A17):

$$h_0 / c = 0.5, \ Str = 0.066, \ C_T = 0.043 \quad \text{and} \quad F_T = 65kN.$$

In the above the Strouhal number is defined as $Str = 2 f_e h_0 / V_S$ and the flapping foil thrust coefficient $C_T = F_T / \left(0.5 \rho V_S^2 S\right)$, where S is the area swept by the vertical oscillatory motion of the foil approximated by $S = 2 h_0 s$. It can be seen in the systematic data presented by Politis & Tsarsitalidis (2015, Fig.A17) that for very low values of Str (as in the present case) the best performance is achieved for quite low values of the self-pitching amplitude. For the purpose of the present study the latter parameter is selected to be θ=6deg, and the estimated performance of the flapping thruster is presented in Fig.8. The previous estimation constitutes a first approximation and does not take into account the exact sectional area of actuation tube of the flapping thruster and the effects of wave orbital velocities. The latter will be treated by future extensions simulating more accurately the dynamical behavior of the system.

The flapping propulsor is expected to reduce the ship responses and the vertical bow motion by 15% (see also Belibassakis & Politis 2013) and also reduce the thrust output by approximately the same level: $F_T = 55kN$. Based on the above calculations, the total resistance is expected to reduce by a quantity 48kN or -12.5% of the calm water resistance at ship speed V_s=17knots. In this case, due to additional thrust provided by the thruster and reduction of wave resistance, the power required from each engine is calculated to decrease to SHP=3955kW. In order to derive data for other wave conditions the data shown in Fig. 8 for the performance of the flapping wave thruster (from Politis & Tsarsitalidis 2015) are systematically used for the estimation dynamic foil thrust coefficient in terms of the Strouhal number $\left(Str\right)$ and the foil heave to chord ratio (h/c).

BULK CARRIER

As second example, we consider a Bulk Carrier of size 7600DWT, with the dimensions L=109m, B=15m, T=7m, and the service speed V_s=14knots. For calculations, the calm water resistance for this hull is estimated using the Formdata systematic series (see, e.g., Harvald 1993) as shown in Fig.9.

Standard propulsion system of Bulk Carrier

A single propeller of diameter D=5m coupled to the main engine is considered. Moreover, the following data are used for the wake fraction and the thrust deduction coefficients, as well as the rotative efficiency and the shafting system efficiency: $1-t=0.84,\ 1-w=0.86,\ \eta_R=1, \eta_S=0.95$. We obtain from this example that for ship speed Vs=14knots the optimally selected propeller pitch ratio is P/D=1.1, which results in SHP=2840kW at 93RPM (propeller revolutions); see Fig.10.

Calculation of B/C responses in waves and flapping system

Working similarly as before, the ship heave and pitch responses are estimated in sea-state conditions 4-5, corresponding to significant wave height Hs=3m and peak period T_p=8sec, and for service ship speed Vs=14knots (Froude number Fn=0.22) in head waves. From the tables provided by Loukakis & Chryssostomidis (1975) and Grigoropoulos et al (2000), we estimate for this ship at sea-state condition 4-5:

vertical bow ship motion with rms amplitude h_0=1.4m,

which provides also a prediction for the heaving amplitude of the bow flapping thruster in waves. We also estimate the following mean value of added wave resistance

R_{add}=80kN at the same ship speed Vs=14knots,

corresponding to about 3.1% of the calm water resistance at the same speed.

For this ship travelling with speed Vs=14knots in head waves with peak period T_p=8sec, the encounter peak frequency is $f_e=0.2$Hz and the corresponding period drops down to 5s. Using a wing with chord c=2.8m and span-to-chord ratio s/c=6 that also fits well in a forward station of the bulk carrier, the Strouhal number of the flapping thruster is Str=0.08. In this condition the behavior of flapping system we obtain the following predictions (see Politis & Tsarsitalidis 2015, Fig.A17)

$$h_0/c=0.5,\ Str=0.08,\ C_T=0.055 \ \text{ and } \ F_T=73kN .$$

The flapping thruster is expected to reduce the ship responses and the vertical bow ship motion by 15% (Belibassakis & Politis 2013), reducing also the thrust output approximately to the same level $F_T=63kN$. Based on the above calculations, the total resistance is expected to drop down by 55.2kN which corresponds to 21% of the calm water resistance at ship speed Vs=14knots. In this case, the power required by the engine is SHP=2155kW and the propeller revolutions 88RPM.

APPLICATION TO A SHIP ROUTE IN THE NORTH SEA

In order to provide predictions of the proposed ship engine and flapping thruster system in waves, a ship route scenario in the North Sea was considered. Based on the density of ship routing from available Marine Traffic - AIS data (https://www.marinetraffic.com/) in the North Sea, a

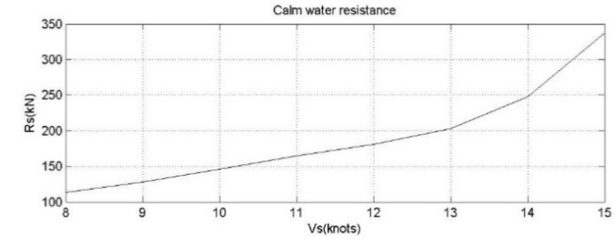

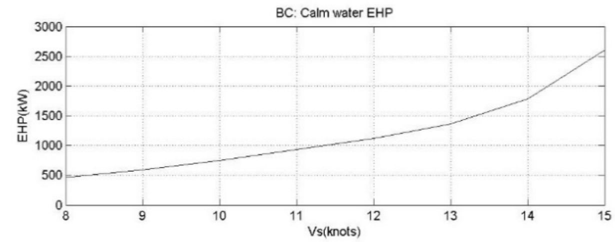

Figure 9. Calm water resistance $R_{cw}(V_s)$ and EHP curves for Bulk Carrier 7600 DWT.

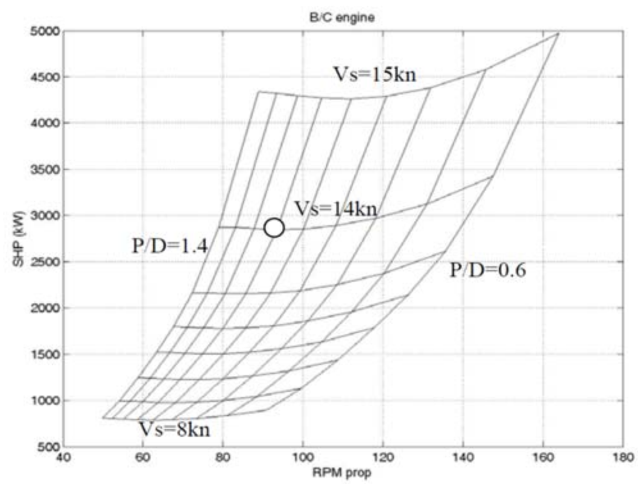

Figure 10. SHP-RPM(prop) diagram for single screw bulk carrier with B4-55 propeller, with propeller pitch-ship speed grid: $0.6 \le P/D \le 1.4$ and ship speed range from $8 \le Vs \le 15$knots. The optimum operating point is indicated by using symbol (SHP=2840kW at 93 RPM propeller).

representative point (55.05degN, 6.5degE) in the southern-central North Sea subregion characterised by very dense marine traffic was selected for the calculations, as shown in Fig.11. For this location, the mean monthly distribution of significant wave height, from MetOcean View (https://app.metoceanview.com/hindcast/sites/nsea/55.05/6.5) is presented in Fig. 12. In conjunction with wave data from FugroGeos (2001) for the Central-Southern North Sea region, the annual mean significant wave height, peak period, standard deviations and the correlation coefficient for the location were estimated as follows:

$\mu_T=T_m$=6.78s, σ_T=1.87, $\mu_H=H_m$=1.69m, σ_H=1.25m, corr.coeff= 0.55.

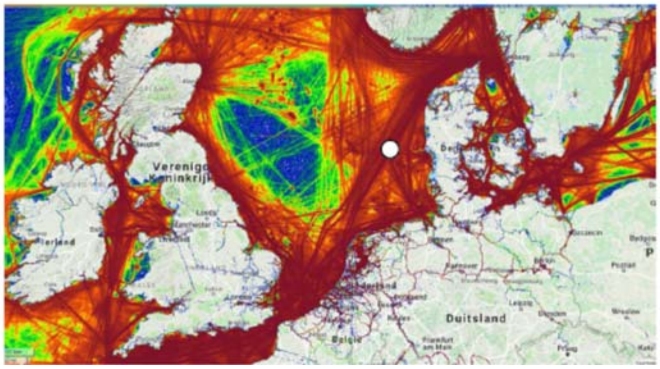

Figure 11. Ship route density of in the North Sea region (from AIS data) and selected reference point (55.05degN, 6.5degE) shown by using dot.

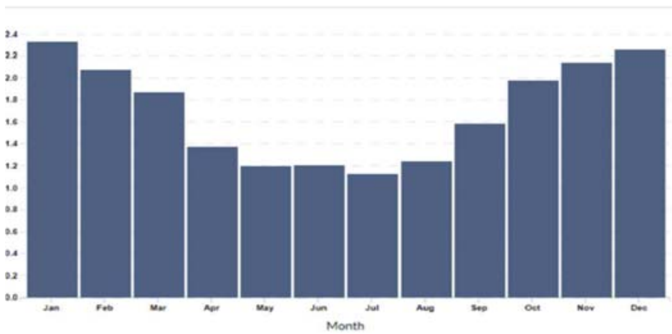

Jan	Feb	Mar	Apr	May	Jun	Jul	Aug	Sep	Oct	Nov	Dec
2,332699	2,066657	1,867803	1,370831	1,198099	1,204164	1,121584	1,23772	1,583213	1,973817	2,138022	2,258667

Figure 12. Mean monthly values of significant wave height at point (55.05° N 6.5° E) in the North Sea region. The annual mean value is H_{m}=1.69m.

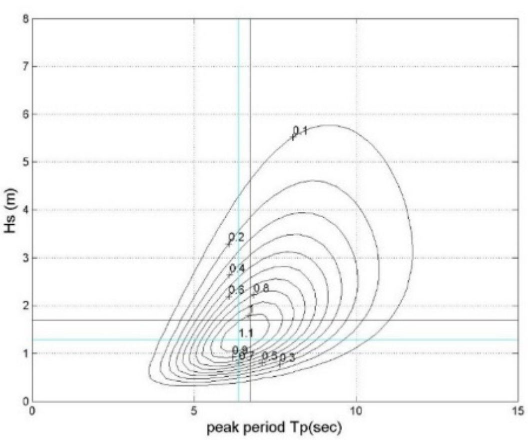

Figure 13. Bivariate lognormal model for the representation of the wave data significant wave height H_S and peak period T_p for the point (55.05° N 6.5° E) in the North Sea region.

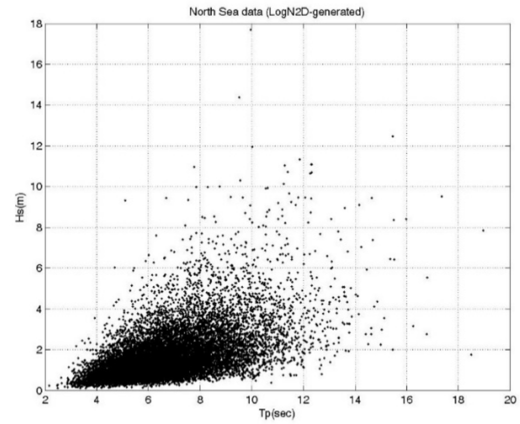

Figure 14. Generated data concerning wave conditions from bivariate logN for significant wave height and peak period for the examined route in the North Sea region.

Following this information a bivariate model of significant wave height and peak period based on the lognormal distribution was derived for the probability density of wave parameters at the specific point as shown in Fig. 13. From this model the most probable wave parameters were determined as: : T_{mpv}=6.37s, H_{mpv}=1.28m, in conjunction with the rest of wave statistics.

Denoting the random variables by $x_1 = T_p,\ x_2 = H_S,$ and the corresponding mean values and standard deviations by μ_{Xk}, σ_{Xk}, respectively, the bivariate lognormal distribution is given by

$$f\left(x_1, x_2\right) = \frac{\exp\left(-\left(u_1^2 + 2\rho u_1 u_2 + u_2^2\right) / \left(2\sqrt{1-\rho_Y^2}\right)\right)}{2\pi x_1 x_2 \sigma_{\mathrm{Y}2} \sigma_{\mathrm{Y}2} \sqrt{1-\rho_Y^2}}, \tag{3}$$

where $u_k = \dfrac{y_k - \mu_{\mathrm{Y}k}}{\sigma_{\mathrm{Y}k}}, k = 1, 2,$ and $y_k = \ln\left(x_k\right),$ while the parameters μ_{Yk}, σ_{Yk}, are obtained as follows:

$$\mu_{\mathrm{Y}k} = \ln\left(\mu_{Xk}\right) - \sigma_{\mathrm{Y}k}^2 / 2, \quad \sigma_{\mathrm{Y}k}^2 = \ln\left(1 + \sigma_{Xk}^2 / \mu_{Xk}^2\right), k = 1, 2, \tag{4}$$

and ρ_Y is the correlation coefficient of the $y_k = \ln\left(x_k\right)$ variables. From the above bivariate pdf model wave data are generated for a large population as presented in Fig.14. As discussed in the previous section, these data are systematically used, in conjunction with (i) propeller performance data, (ii) ship responses and wave added resistanse from systematic series from, and (ii) flapping thruster performance presented in Fig.8, in order to calculate ship engine performance in head waves, with and without the flapping foil thruster for the whole population of wave conditions.

On the basis of the calculated results the expected improvement by the operation of the biomimetic wave thruster for varius sea states represented by values of the signifficant wave height is calculated as shown in Fig.15, in the case of (a) the ROPAX 120m ship for the service speed Vs=17kn, and (b) the Bulk Carrier also for the service speed Vs=14kn, for the given location in the North Sea.

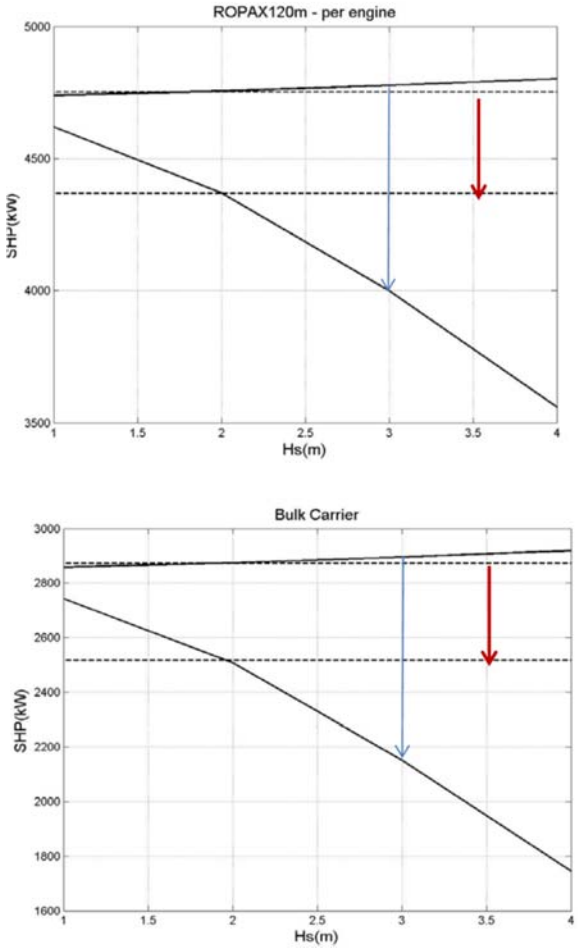

Figure 15. Simulation of the performance of ship engine, in complementarity with biomimetic flapping thruster.

In these plots the upper solid lines indicate the increase of calculated SHP (in kW per engine) due to the waves and the lower solid line the expected improvement due to the operation of the biomimetic thruster in waves shown by using an arrow. In addition, red arrows indicate the overall expected enhancement in the interval of 0.25m<*H*s<4m. As a first estimation at the ship service speed we obtain that the overall expected performance enhancement ranges from 8% (ROPAX ferry) to 12% (BC), while for *H*s=3m the enhancement is from 16% (ROPAX ferry) to 25% (BC). For both ship-types considered the above calculations are extended for various ship speeds: (a) for *V*s=15,17,19kn, concerning the ferry, and (b) for *V*s=12,14,15kn for the Bulk Carrier and the results are presented in Figs.16 and 17, respectively. These figures show the corresponding operation points on the engine power - propeller rpm diagram. In the latter subplots the effect of sea-state condition, as represented by the significant wave height, is illustrated by using color dots on the propeller curves corresponding to the ship speeds considered. The data above the values corresponding to the calm-sea condition correspond to the increase of power due to the added wave resistance effect. On the other hand, the data on the propeller curves below the calm condition indicate the improvement of performance due to the operation of the dynamic flapping wing thruster. The line indicated by using a cyan-colored curve on the ship engine power – propeller rpm subplots corresponds to

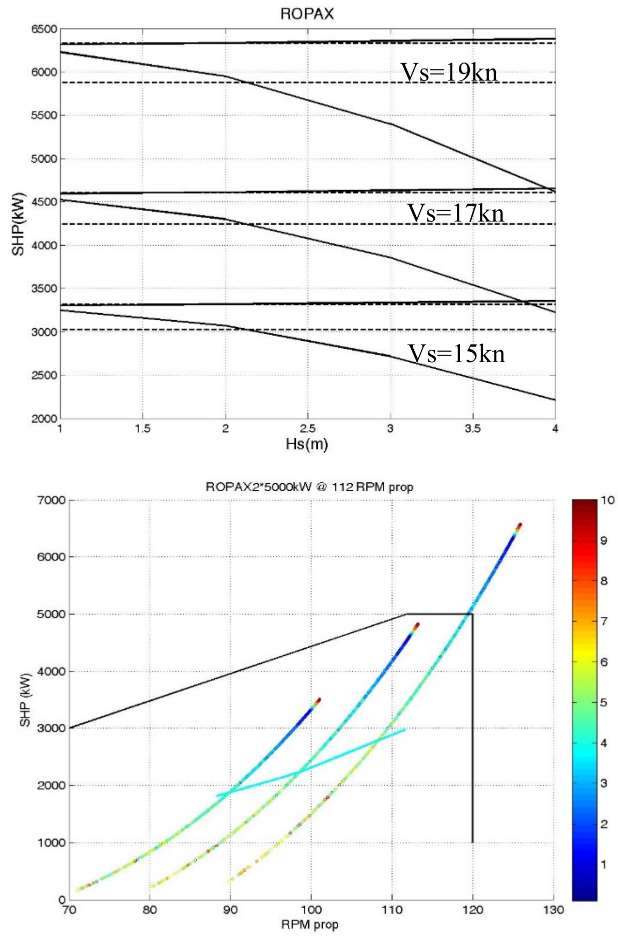

Figure 16. Estimation of the performance of each ferry ship engine, with and without the biomimetic flapping thruster, for ship speeds *V*s=15kn,17kn,19kn, in various sea states indicated by using color for the value of the signifficant wave height.

a sea state with significant wave height H_s=5m, considered as an upper limit from the point of view of strength and safety requirements for the operation of the biomimetic thruster in waves.Taking into account that the present results contain an error associated with the cumulative inaccuracy of application of systematic series data, they constitute first indication and trends of the performance of the flapping thruster in waves in combination with the ship engine-propulsion system. It is shown that the use of flapping foils could augment the overall propulsive efficiency of ships and reduce engine load by extracting energy from the waves (and simultaneously damping the oscillatory ship motions). The above effect is more signifficant in moderate to high sea conditions, while in extreme weather conditions a retraction mechanism for the dynamic foil system may be required to avoid damage. The concept shows significant promise and is likely to be applicable to a wide range of ship types.

CONCLUSIONS

Flapping foil thrusters arranged at the bow of ships travelling at constant forward speed in waves could be exploited for augmenting the

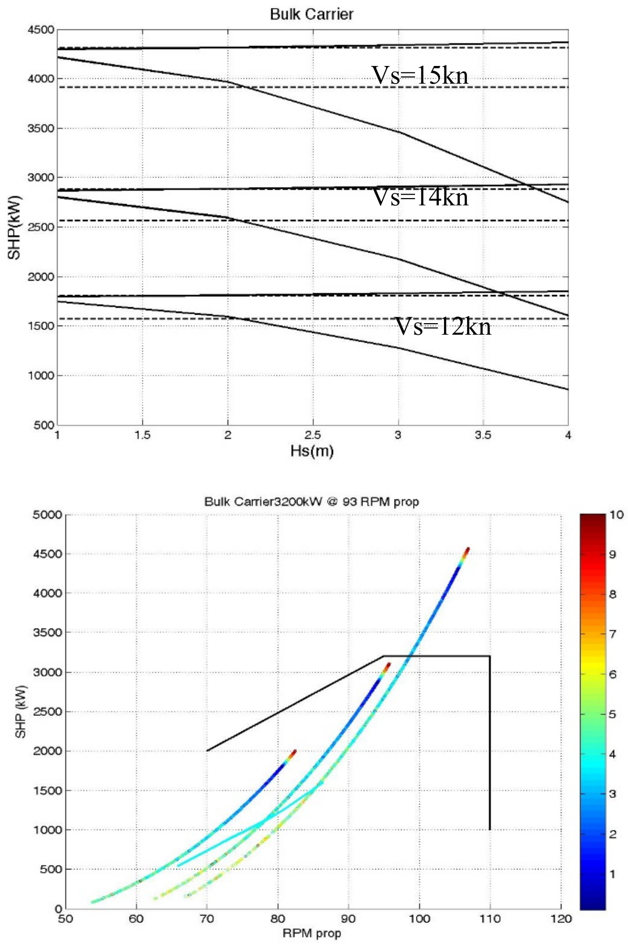

Figure 17. Estimation of the performance of BC ship engine, with and without the biomimetic flapping thruster, for ship speeds *V*s =12kn, 14kn and 15kn, in various sea states indicated by using color for indicate the signifficant wave height

overall propulsion in waves by directly converting kinetic energy from ship motions to thrust and improving dynamic stability. Based on simplified ship and foil dynamics models, in conjunction with ship engine data a short-sea shipping scenario in the North Sea for a passenger-car ferry and bulk carrier was presented, illustrating the complementary nature of dynamic wing and engine innovations. The results show that the additional thrust generated by the dynamic wing will enable the engine to operate in part-load without compromising vessel speed, resulting in an additional positive effect on its emission profile. Future work is planned towards the development of more accurate methods for the prediction of short-time and long-time combined dynamics of ship engine – biomimetic thruster performance in waves for a variety of ship types.

ACKNOWLEDGEMENTS

This project has received funding from the European Union's Horizon 2020 research and innovation programme under grant agreement No 857840

The opinions expressed in this document reflect only the author's view and in no way reflect the European Commission's opinions. The European Commission is not responsible for any use that may be made of the information it contains.

REFERENCES

Belibassakis K.A., Politis G.K., 2013, Hydrodynamic performance of flapping wings for augmenting ship propulsion in waves, *Ocean Engineering* 72, 227-240.

Belibassakis K.A., Filippas, E., 2015, Ship propulsion in waves by actively controlled flapping foils, *Applied Ocean Research* 52, 1–11.

Bøckmann, E., Steen, S. 2014, Experiments with actively pitch-controlled and spring-loaded oscillating foils. *Applied Ocean Research.* 48, pp. 227–235

Bøckmann, E., Steen, S., 2016, Model test and simulation of a ship with wavefoils. *Applied Ocean Research* 57, 8–18.

Bowker J., Tan M., Townsend, N., 2020, Forward speed prediction of a free-running wave-propelled boat, *IEEE Journ.Oceanic Engin.*, DOI10.1109/JOE.2020.2990143.

Filippas E., Papadakis, G., Belibassakis K.A., 2020, Free-Surface Effects on the Performance of Flapping-Foil Thruster for Augmenting Ship Propulsion in Waves, *Journal Marine Science & Engineering, 8*(5), 357.

FugroGeos, 2001, Wind and wave frequency distributions for sites around the British Isles Offshore Technology Report 2001/030.

Grigoropoulos G.J., Loukakis T.A., Perakis A.N., 2000, Seakeeping standard series for oblique seas, *Ocean Engineering* 27, 111–126

Harvald S.,1983, *Resistance and propulsion of ships*, Wiley.

Lewis EV. 1988, *Principles of Naval Architecture.* Soc. Naval Architects & Marine Eng. (SNAME). New Jersey.

Loukakis, T.A., Chryssostomidis, C., 1975. Seakeeping standard series for cruiser-stern ships. *Transactions SNAME* 83, 67–127.

Naito, S.; Isshiki, H. 2005, Effect of bow wings on ship propulsion and motions. *Appl. Mech. Reviews* 58(4), 253-268.

Politis G.K., Tsarsitalidis V.T., 2014, Flapping wing propulsor design: An approach based on systematic 3D-BEM simulations *Ocean Engineering* 84, 98-123.

Rozhdestvensky, K.V.; Ryzhov, V.A. 2003, Aero-hydrodynamics of flapping wing propulsors. *Progress in Aerospace Sciences* 39, 585-633.

De Silva LWA, Yamaguchi H. 2012, Numerical study on active wave devouring propulsion. *J Mar Sci Technol*. 17:261–75

Triantafyllou, M.S., Triantafyllou, G.S., Yue, D.K.P., 2000, Hydrodynamics of fishlike swimming. *An. Review Fluid Mech*. 32, 33-53.

Triantafyllou, M.S., Techet, A.H., Hover, F.S. 2004, Review of experimental work in biomimetic foils. *IEEE J. Oceanic Eng.* 29, 585-594.

Taylor, G.K., Triantafyllou, M.S., Tropea C., 2010, *Animal Locomotion* Springer.

Vermeiden J., Kooiker K., Lafeber F.H., van Terwisga T., Cerup-Simonsen B., Folsø R., 2012, A Systematic Experimental Study on Powering Performance of Flapping Foil Propulsors, Proc. 29th *Symp. Naval Hydrodynamics*, Gothenburg, Sweden.

Wu, X., Zhang, X., Tian, X., Li, X., Lu, W. 2019, A review on fluid dynamics of flapping foils. *Ocean Engineering,* doi: 10.1016/j.oceaneng.2019.106712.